Tetrahedron Green Chem 5 (2025) 100070

Contents lists available at ScienceDirect

Tetrahedron Green Chem

journal homepage: www.journals.elsevier.com/tetrahedron-green-chem

Protecting group-free photocatalyzed *O*-arylation of quinic acid

Miguel A. Bárbara [a], Nuno R. Candeias [b,c,*], Luis F. Veiros [d], Filipe Menezes [e], Andrea Gualandi [f,g], Pier G. Cozzi [f], Carlos A.M. Afonso [a,**]

[a] Research Institute for Medicines (iMed.ULisboa), Faculty of Pharmacy, Universidade de Lisboa, Av. Prof. Gama Pinto, 1649-003, Lisbon, Portugal
[b] LAQV-REQUIMTE, Department of Chemistry, University of Aveiro, 3810-193, Aveiro, Portugal
[c] Faculty of Engineering and Natural Sciences, Tampere University, Korkeakoulunkatu 8, 33101, Tampere, Finland
[d] Centro de Química Estrutural, Institute of Molecular Sciences, Departamento de Engenharia Química, Instituto Superior Técnico, Universidade de Lisboa, Av. Rovisco Pais, 1049 001, Lisboa, Portugal
[e] Helmholtz Munich, Molecular Targets and Therapeutics Center, Institute of Structural Biology, Ingolstädter Landstr. 1, 85764, Neuherberg, Germany
[f] Dipartimento di Chimica "Giacomo Ciamician", Alma Mater Studiorum—Università di Bologna, Via Gobetti 85, 40129, Bologna, Italy
[g] Center for Chemical Catalysis – C3, Alma Mater Studiorum – Università di Bologna, Via Gobetti 85, 40129, Bologna, Italy

ARTICLE INFO

Keywords:
Quinic acid
Photoredox
Polyols
Coupling
DFT calculations
Photocatalysis

ABSTRACT

This study presents a novel and environmentally friendly approach to the preparation of quinic acid-derived esters from photocatalyzed *O*-arylation with haloarenes. This study expands the quinic acid-derived chemical space from renewable biomass by harnessing the power of visible-light-driven photocatalysis under mild conditions without the need for protecting groups. A thorough screening of reaction conditions, including the choice of photocatalyst, solvent, base, nickel source, and ligand, led to the identification of the most effective conditions, these being 5CzBN as the optimal photocatalyst, and glyme-based nickel complexes as the preferred nickel source. These conditions enabled the formation of *O*-arylated products with good yields without noticeable formation of decarboxylated products. Computational calculations support the proposed mechanism for the *O*-arylation process, based on oxidative addition, anion exchange, and reductive elimination upon energy transfer from the photocatalyst to the Ni(II) species. Computational considerations for a nickel-catalyzed photodecarboxylative arylation mechanism suggest that the oxidation of quinate by the excited photocatalyst or other species derived thereof is considerably less favorable than a pathway only involving energy transfer to a nickel species. The research provides valuable insights into the mechanism of this environmentally conscious transformation.

1. Introduction

Highly functionalized biomass-derived molecules can be taken as interesting starting materials for fine chemical synthesis, from which the exploration of the chiral pool stands out as a particularly relevant example [1]. The amalgamation of the chiral pool concept into biorefinery operations [2] offers a distinct advantage by leveraging the inherent enantioselectivity of naturally occurring compounds, facilitating the development of novel catalysts [3] and engendering innovative synthetic strategies [4]. This synergy eases the production of enantiomerically pure valuable chemicals and pharmaceuticals [5], thereby contributing to the advancement of a more sustainable and eco-conscious chemical industry.

Quinic acid (QA), a secondary metabolite derived from the shikimate pathway, holds a ubiquitous presence in both plant and microorganism kingdoms. This cyclic polyhydroxy compound manifests as a sole stereoisomer in various plant barks, tobacco leaves, carrot leaves, apples, peaches, coffee seeds, and food wastes [6]. Viewed through the lens of sustainability, endeavors to employ QA as a viable raw material for generating benzoic acid [7] and other aromatics [8] have encountered obstacles due to the high cost of its bacterial production from glucose [9]. However, the recent advances in modifying microorganisms for the biosynthesis of quinic and shikimic acids offer a prospective avenue for broadening the chemical space derived from biomass [10].

* Corresponding author. LAQV-REQUIMTE, Department of Chemistry, University of Aveiro, 3810-193, Aveiro, Portugal.
** Corresponding author. Research Institute for Medicines (iMed.ULisboa), Faculty of Pharmacy, Universidade de Lisboa, Av. Prof. Gama Pinto, 1649-003, Lisbon, Portugal.
E-mail addresses: ncandeias@ua.pt (N.R. Candeias), carlosafonso@ff.ulisboa.pt (C.A.M. Afonso).

https://doi.org/10.1016/j.tgchem.2025.100070
Received 27 November 2024; Received in revised form 21 February 2025; Accepted 21 February 2025
Available online 22 February 2025

Despite the extensive exploration of QA as a starting material in synthetic chemistry, which has yielded foundational directives for its synthetic manipulation [11], the high number of OH-containing functional groups within its compact structure presents substantial challenges in achieving selectivity. One of the often-used protections is the carboxylic acid conversion to an ester, which allows the modification of the hydroxy groups and facilitates the manipulation of the cyclic polyol. The structural features of QA, in which one of the chair conformations is described by the proximity of the carboxyl group with the 5-OH, make it very easy to form the lactone derivative known as quinide. While this is the most often used strategy when the protection of the 5-OH is also desirable, the single modification of the carboxylic acid to an ester is challenging. Indeed, the esterification of QA is typically performed in the presence of strongly acidic conditions using methanol or ethanol as nucleophiles and as a solvent, most likely through a quinide intermediate (Scheme 1a). Scarce examples from the literature report the use of the carboxylate salt as a nucleophile in nucleophilic substitutions with alkyl halides, namely benzyl chloride, or its *para*-nitro derivative [12], 6-bromomethyl-1,4-anthracenedione [13], or 6-bromo-1-hexene [14]. A literature survey shows that the selective manipulation of the QA's carboxyl functionality towards esterification is very limited to introducing primary alkoxyl substituents, as coupling agents tend to lead to intramolecular esterification [15].

Photoredox catalysis has witnessed a remarkable renewed interest for synthetic chemists over the last decade [16]. Harnessing visible light to drive redox reactions is remarkable from a sustainable perspective [17], as the use of light is less energy-intensive, often requiring milder conditions and being more selective than traditional methods. Additionally, greener solvents, such as water, that is often associated with undesired reactivities, can be used due to their inertness towards open shell reactive intermediates [18]; the shuttle of electrons between species, often not requiring the stoichiometric reagents to effectively change the substrates' oxidation states, greatly contributes to a better atom economy of the transformations. The appealing properties of photoredox catalysis in regards to its sustainability has motivated vibrant research on its use for the manipulation of biomass derived molecules [19].

The traceless extrusion of CO_2 from carboxylic acids allows building a myriad of C–C bonds starting from different carbon hybridization states [20]. Only recently, the extension of photochemical decarboxylative arylation was significantly expanded to tertiary carboxylic acids (Scheme 1b) [21], after studies on the influence of additives by Dreher and MacMillan [22]. Instead, the formation of *O*-arylated esters from carboxylic acids and aryl halides using photoredox catalysis has been reported either intentionally [23] or as a side path for the decarboxylative light-mediated C(sp^3)-C(sp^2) cross-coupling (Scheme 1b) [24]. The divergent metal-free photochemical pathway was also studied [25], whilst nickel's redox promiscuity was reported to promote the light-free formation of reactive species [26].

Considering the large abundance of QA (and its corresponding esters) in nature, it was envisioned that the light-driven modification of QA could provide an opportunity to generate an open shell reactive intermediate prone to functionalization. Of particular interest would be the possibility of selectively arylating the oxygen of the carboxylic acid moiety without resorting to any hydroxyl-protecting groups. The merge of nickel catalysis, using bipyridyl ligands, and photoredox catalysis has been considered a unique method to *O*-arylate the carboxylic acid without interference with the lactonization process (Scheme 1c). In this work, we set to showcase the *O*-arylation of QA, demonstrating that, despite the presence of the multiple hydroxyl functionalities, the nickel complexes are taken in the selective formation of a new C(sp^2)-O(sp^3) bond. This work seminally reports the preparation of quinic acid-derived *O*-aryl esters, bypassing the use of phenol derivatives and thus avoiding the competitive formation of quinide lactone. The influence of several key experimental parameters, such as photocatalyst, solvent, base, nickel ligands, and additives, was investigated. The necessity of protecting the QA's hydroxyl groups was also evaluated due to its utmost importance for the valorization of natural resources. A thorough

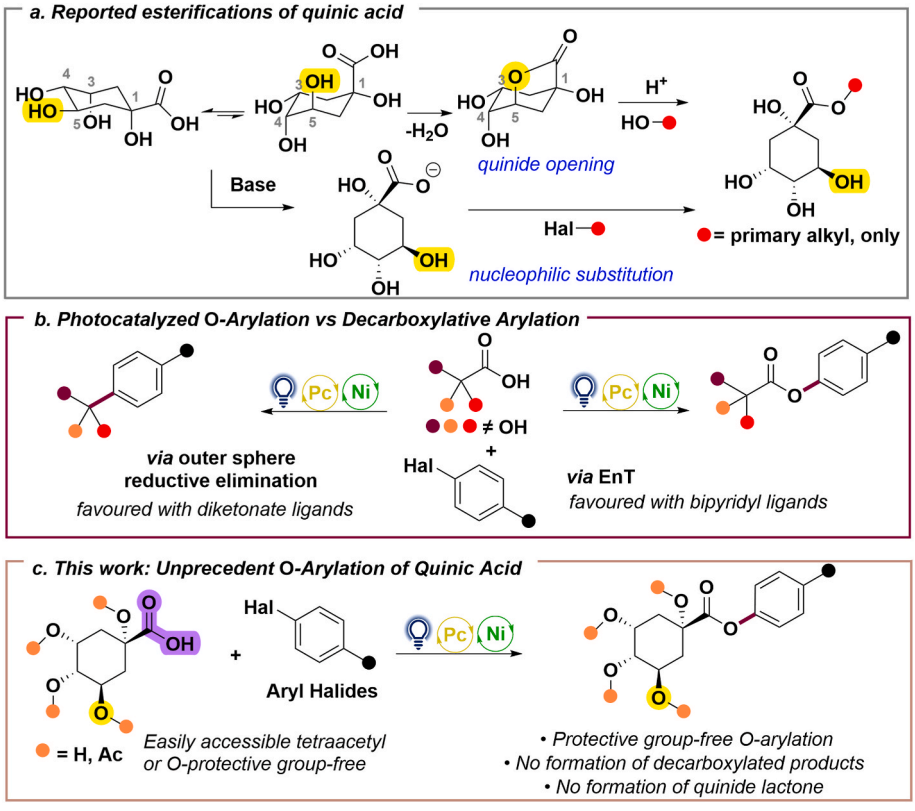

Scheme 1. a) Esterification of QA. b) Tertiary carboxylic acids in merged photoredox and nickel catalysis. c) Photoredox modification of QA.

computational study on DFT calculations is also presented to justify the selectivity of the transformation by comparing the *O*-arylation with the photodecarboxylative arylation process.

2. Results and discussion

We commenced the *O*-arylation of QA by screening the photocatalyst, in the presence of 2-*tert*-butyl-1,1,3,3-tetramethylguanidine (btmg) as a base, nickel bromide glyme and 2,2′-bypyridine (bpy) to form the metal complex catalyst, and in DMSO to ensure the complete solubilization of QA. The initial choice of the photocatalyst was based on its ability to reduce nickel(II) to nickel(0), this result was expected according to the redox potentials of the excited state photocatalyst. Impelled by the previous reports on the use of iridium photosensitizers and nickel complexes [27], and by the use of phthalimide to slow down the nickel-catalyzed protodehalogenation pathway of aryl halides [22], we started our screening by employing 1 mol% of a heteroleptic iridium (III) photocatalyst Ir[dF(CF_3)ppy]$_2$(dtbbpy)PF_6 to gladly observe the formation of the highly congested *O*-arylation product in 70 % yield (Table 1, entry 1). The same photocatalyst was deemed suitable for the combination with nickel chloride (entry 7), whilst its non-fluorinated congener provided the same product in a reduced 54 % yield (entry 2). The homoleptic Ir(dFppy)$_3$ promoted the formation of the desired product in 61 % yield (entry 3). Notwithstanding the success of the use of iridium complexes, we decided to focus on organic dye due to their smaller environmental impact when compared with their metallic counterparts. When using $NiBr_2$.glyme as the transition metal catalyst, 4CzIPN and 5Czbn showed very similar results (64 % and 66 % ^{1}H NMR yield respectively, entries 5–6). Despite the similar profile of redox potentials of cyanobenzene-based photosensitizer 3DAPFIPN, its use resulted in much lower yield (25 % ^{1}H NMR yield, entry 4). Curiously, when using nickel chloride glyme, no reaction was observed (entry 8), whilst the pentacarbazole derivative penta-carbazolylbenzonitrile (5CzBN) could deliver the product in 64 % and 72 % yields from nickel bromide (entry 6) and chloride (entry 9), respectively. These observations are in accordance with the MacMillan [23] proposal of the energy transfer phenomenon being the driving force of this reaction. Indeed, the energy of the lowest triplet state (E_T) of 5CzBn is higher than the one reported for 4CzIPN [28]. Unfortunately, such energy data for E_T of 3DPAFIPN is not available, nevertheless the photocatalyst was proven to be unstable under irradiation [29].

After identifying 5CzBN as the best photocatalyst, we turned our attention to the nickel source and its ligand. Keeping the 4,4′-bis(*tert*-butyl)-2,2′-bipyridine (dtbbpy) as the nickel ligand, different nickel sources were screened (Table 2, entries 1–6). Moving from $NiBr_2$ (entry 2) to the glyme complex improved only slightly the yields (entries 1 and 3). Ni(acac)$_2$ was observed to behave similarly to $NiBr_2$ (entries 2 and 4) while changing to the air-sensitive Ni(cod)$_2$ resulted in a decreased yield by 11 % and complete lack of reaction in the absence of nitrogenated ligand (entries 5 and 6). Similar reactivity was observed for the diketonate Ni(acac)$_2$ (entry 2) in comparison with other nickel sources, which seems to point to a high propensity of the QA derivative to avoid decarboxylation under those conditions [21]. Screening of the nickel ligands (Table 2, entries 7–11) has shown that the unsubstituted bipyridine and its 4,4′-dimethyl congener were effective in stabilizing the metal complex to promote the formation of the desired product (entries 7 and 8). On the other hand, the electron-rich 4-4′-dimethoxy-2-2′-bipyridine (4,4′-dMeObpy) proved to be similar to dtbbpy (entry 9). More restricted phenanthroline and neocuproine ligands were identified as detrimental to the reaction success (entries 10 and 11). The amount of photocatalyst could be reduced to 1 mol% by either increasing the amount of QA and base (entry 13) or aryl iodide (entry 14). Finally, the photocatalyzed *O*-arylation of the protecting group-free QA could be tuned to 85 % yield by increasing the amount of QA and base to 2 equivalents (entry 15). The need for ligand (entry 16), photocatalyst (entry 17), and light (entry 18) to achieve product formation was confirmed.

Upon establishing the conditions for the direct use of protecting group-free QA in the *O*-arylation procedure, we set to study the scope of the transformation. Considering the lack of solubility of QA in most organic solvents, the easy-to-prepare tetraacetyl quinic acid (**TAQA**) was used in further studies, thus allowing screening of other solvents. $NiCl_2$•glyme was kept in the scope evaluation as it proved to be a better nickel source when using QA. On the other hand, while other bipyridines

Table 1
Photocatalyst screening.

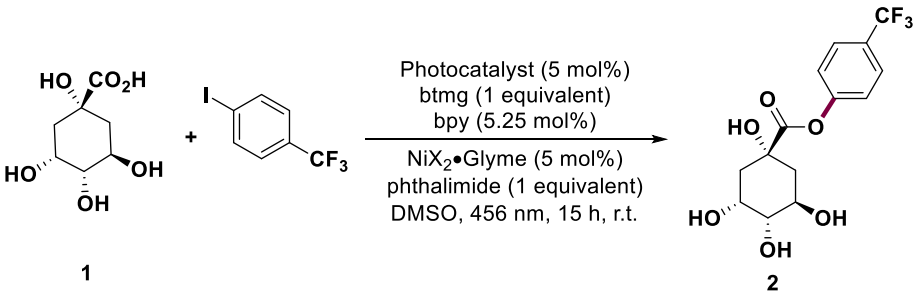

Entry[a]	Photocatalyst	X	Yield (%)[b]*
1	(Ir[dF(CF_3)ppy]$_2$(dtbbpy))PF_6[c]	Br	70
2	[Ir(dtbbpy)(ppy)$_2$]PF_6	Br	54
3	Ir(dFppy)$_3$	Br	61
4	3DPAFIPN	Br	25
5	4CzIPN	Br	66
6	5CzBN	Br	64
7	(Ir[dF(CF_3)ppy]$_2$(dtbpy))PF_6[c]	Cl	57
8	4CzIPN	Cl	nr[d]
9	5CzBN	Cl	72

[a] 50 μmol of QA and 50 μmol of iodoarene were used in 0.5 mL DMSO-d_6, according to the general procedure.
[b] Determined by ^{1}H NMR using 1,3,5-trimethoxybenzene as internal standard.
[c] 1 mol % of photocatalyst.
[d] nr = no reaction.

Table 2
Nickel source and ligands screening.

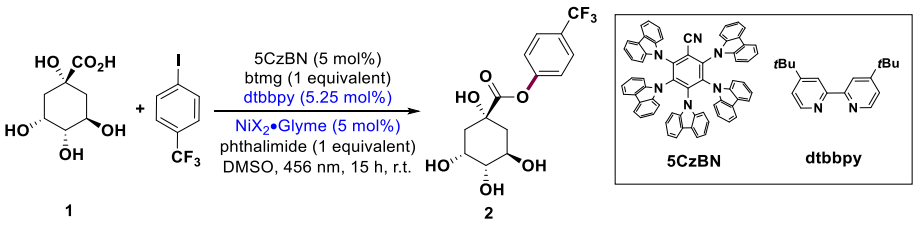

Entry[a]	Modification	Yield (%)[b]
1	X = Br	61
2	$NiBr_2$ instead of NiX_2·glyme	60
3	X = Cl	63
4	$Ni(acac)_2$ instead of NiX_2·glyme	62
5	$Ni(cod)_2$ instead of NiX_2·glyme	11
6	$Ni(cod)_2$ instead of NiX_2·glyme and no ligand	nr[c]
7	X = Br, bpy instead of dtbbpy	81
8	X = Br, dmbpy instead of dtbbpy	80
9	X = Br, 4,4′-dMeObpy instead of dtbbpy	69
10	X = Br, *o*-phenanthroline instead of dtbbpy	56
11	X = Br, neocuproine instead of dtbbpy	17
12	X = Cl, 1 mol% of 5CzBN	52
13	X = Cl, 1 mol% of 5CzBN and 2 equiv of QA and btmg	69
14	X = Cl, 1 mol% of 5CzBN and 2 equiv of aryl iodide	60
15	X = Cl, 2 equiv of QA and 2 equiv of btmg	85
16	X = Cl, no ligand	nr[c]
17	X = Cl, No photocatalyst	nr[c]
18	X = Cl, No light	nr[c]

[a] 50 μmol of QA and 50 μmol of iodoarene were used in 0.5 mL DMSO-d_6, according to the general procedure for quinic acid *O*-arylation.
[b] Determined by ^{1}H NMR using 1,3,5-trimethoxybenzene as internal standard.
[c] nr = no reaction.

were superior to dtbbpy, the latter was kept in the following task due to its solubility in a wider range of solvents. Upon tweaking the stoichiometry, different bases (entries 1–5) and solvents (entries 6–15) were screened for the arylation of **TAQA** (Table 3). Amongst the three bases considered, btmg and ^{t}BuOK resulted in similar yields of the desired product (entries 1–3), whilst Cs_2CO_3 resulted in considerably lower formation of the product in only 11 % yield (entry 4). Besides the noticeable effect of the base, the presence of phthalimide as an additive proved beneficial for the reaction's success, as in its absence, the product could not be formed in more than 18 % yield (entries 2 and 5). The effect of the solvent was a determinant factor for the reaction success since using less polar solvents was generally detrimental to the reaction yield, resulting in the product formation of up to 50 % yield for THF (entry 8). Whilst the use of DMF, NMP, and DMA led to product formation in similar yields, in the 58–65 % range (entries 1, 10 and 14), the use of methanol resulted in no reaction due to the lack of solubility of the photocatalyst (entry 11). Using water as solvent was even more limited regarding the reactants' low solubility. Acetonitrile leads to the formation of the arylated product in only 28 % yield (entry 13). Despite our endeavor to find an alternative solvent for the arylation of **TAQA**, which could simplify the work-up and isolation of the intended products, DMSO remained the best solvent, allowing for the formation of the desired product in 72 % yield (entry 15), comparable to the procedure described for the direct modification of protecting group free QA. Doubling the number of equivalents of TAQA allowed substantial increase of the yield, resulting in formation of product in 86 % (entry 16). Despite the extended conversions observed by TLC and ^{1}H NMR of the crude mixtures, isolation of the product invariably resulted in decreased yields due to their considerable water solubility and lack of stability in silica. Nevertheless, product **4a** could be obtained in 45 % yield from 0.2 mmol of the aryl iodide after aqueous work-up, as determined by ^{1}H NMR using 1,3,5-trimethoxybenzene as internal standard.

The scope of the transformation was further assessed to consider both iodo- (Scheme 2a) and bromoarenes (Scheme 2b), with the yields depending mostly on the electronic nature of the aryl halide. Unsurprisingly, the presence of electron-withdrawing groups in the aryl halide partner was beneficial for the reaction success, a limitation already shown for photoredox decarboxylative arylation [22,30], attributed to the oxidative addition being the turnover-limiting step [31]. Besides the introduction of aryl rings with one (**4a**) or multiple trifluoromethyl moieties (**4b**), the reaction was also amenable to the introduction of aryl nitriles (in either *o*- and *p*-positions – **4c** and **4g**), acetophenones (simple and α-brominated – **4d** and **4h**), a *m*-carboxylic ester (**4f**), and polycyclic aromatic moieties (**4e, 4i** and **4j**). Despite our multiple attempts to introduce electron-rich aryl partners (Scheme 2c), the reaction failed to provide the desired compounds. Similarly, the use of iodobenzene led to the formation of products with low yield, which was also verified for two dicarbonyl compounds (Supporting Information). Considering that the electronic structure of Ni-bpy species is highly sensitive to both ligands and the surrounding environment [32], employing other bipyridyl ligands [33] is an envisioned approach to expand the transformation to the use of electron-rich aryl halides. Notwithstanding the moderate yields reported in Scheme 2, the preparation of quinic acid-derived *O*-aryl esters, either using *O*-protecting groups or not, has not been unequivocally reported before [34]. Furthermore, apart from the simple preparation of methyl or ethyl quinate esters, the installation of other longer alkyl primary substituents starting from quinic acid usually proceeds in only moderate yields (30–58 %) [12,13].

2.1. Computational study

Numerous studies on the nickel photoredox esterification of aryl halides support an energy transfer process between the photocatalyst and a nickel species [35], as initially reported by MacMillan [23]. In

Table 3
Optimization of TAQA photoredox esterification.

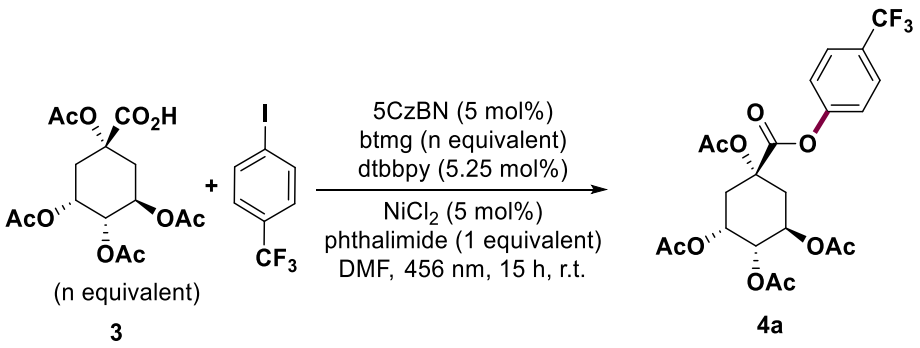

Entry	n equivalent[a]	Modification	Yield (%)[b]
1	1 or 1.5	None	60
2	1.5	^{t}BuOK as base	41
3	1.5	^{t}BuOK as base in DMSO	24
4	1.5	Cs_2CO_3 as base	11
5	1.5	^{t}BuOK as base, no phthalimide	18
6	1	Toluene as solvent	31
7	1	EtOAc as solvent	21
8	1	THF as solvent	50
9	1	Acetone as solvent	35
10	1	NMP as solvent	58
11	1	MeOH as solvent	n.r.[c]
12	1	THF/MeCN (1:1) as solvent	56
13	1	MeCN as solvent	28
14	1	DMA as solvent	65
15	1	DMSO as solvent	72
16	2	DMSO as solvent	86 (45 %)[d]

[a] 1 mL of solvent and 0.1 mmol of iodoarene was used, according to the general procedure as indicated for quinic acid *O*-arylation.
[b] Determined by ^{1}H NMR using 1,3,5-trimethoxybenzene as internal standard, according to conditions used for Table 2.
[c] nr = no reaction.
[d] Yield determined by ^{1}H NMR using 1,3,5-trimethoxybenzene as internal standard, from 0.2 mmol of aryl iodide, according to general procedure for TAQA *O*-arylation.

order to ascertain that possibility when using QA, we undertook a density functional theory study at the BP86(PCM-DMSO)/(SDD, 6-31+G**) level of theory. A full account of the computational details is presented as Supporting Information. The choice of the BP86 method is justified by the good description of the spin-state splitting for first-row transition metals [36]. Intrigued by the lack of formation of decarboxylative arylation products and considering that different mechanism pathways can be followed depending on the nature of the ketyl radical or subtle changes in the nickel ligand [21,37], the *O*-arylation mechanism was compared with a hypothetical decarboxylative arylation mechanism based on the literature precedents [21,30–32,38] (see Supporting Information). Moreover, **5CzBN** has scarcely been considered a competent photocatalyst, and to the best of our knowledge, this is the first report on its use for the *O*-arylation of carboxylic acids.

The study started by considering the formation of a Ni(0) species from Ni(II), analogously to the process with iridium complexes as photocatalysts [27,35b,39]. The nickel ligand dtbbpy was replaced by the simpler 2,2′-bipyridine for the sake of computational cost, and 4-iodobenzotrifluoride was used as the haloarene partner for the energy profile presented in Fig. 1. The oxidative addition step was determined to be exergonic ($\Delta G = -26.1$ kcal/mol), with a small energy barrier of only 1.9 kcal/mol to reach **TS1**‡. This results from an electron-rich metal and a coordinatively unsaturated species combined with the electron deficiency of 4-iodobenzotrifluoride and the rather weak carbon-iodine bond. Bringing the btmg and QA pair close to the square planar nickel (II) complex **6** is unfavorable due to the entropy contribution (by 7.6 kcal/mol). Unsurprisingly, the proton exchange process between QA and btmg is also exergonic with $\Delta G = -14.4$ kcal/mol, measured from **7** to **8**. It starts with transition state **TS2**‡, in which the nickel complex is merely a spectator species in a process with a negligible barrier of 1 kcal/mol at the electronic level. **TS2**‡ is characterized by the proton transposition from QA into the sp^2 nitrogen of guanidine, while an additional hydrogen bond of 1.82 Å, established between the α-hydroxyl and the sp^2 nitrogen, stabilizes the transition state. The carboxylate of species **8** is stabilized by an intramolecular hydrogen bond with the α-hydroxyl group and taken by the nickel complex for anion exchange with iodide. The energy barrier is again small, of only 4.5 kcal/mol to reach the trigonal bipyramidal **TS3**‡, having the incoming and outcoming ligands at equatorial positions at an angle of 102°. The transition state **TS3**‡ is characterized by the establishment of the Ni–O bond ($d_{Ni\text{-}O}$ = 2.13 Å) and elongation of the Ni–I bond ($d_{Ni\text{-}O}$ = 2.53 Å in **8** vs $d_{Ni\text{-}O}$ = 2.76 Å in **TS3**‡). Removal of the guanidinium iodide derivative from the mixture results in a stable quadrangular Ni(II) complex, ^{S}**10**, that requires 35.9 kcal/mol to overcome the reductive elimination energy barrier, corresponding to the rate determining step. When considering an energy transfer pathway, which involves the decay of the excited triplet photocatalyst to the singlet ground state **5CzBN**, the high spin distorted tetrahedral complex ^{T}**10** can be reached and undergo reductive elimination through a less energy-demanding pathway of 27.9 kcal/mol. The transition state is described by the incipient formation of a C–O bond between the arene and the carboxylate ($d_{C\text{-}O}$ = 1.76 Å) while the nickel atom keeps its distance from the arene's carbon ($d_{Ni\text{-}C}$ = 1.97 Å in ^{T}**TS5**‡ vs $d_{Ni\text{-}C}$ = 1.95 Å in ^{T}**10**). The geometry ^{T}**11** corresponds to the establishment of a more solid O–C bond ($d_{C\text{-}O}$ = 1.46 Å) with the arene and weakening of the Ni–C bond ($d_{Ni\text{-}C}$ = 2.07 Å). The energy transfer process from the triplet photoexcited state **5CzBN*** to ^{S}**10** is an endergonic process ($\Delta G_{EnT} = -29.6$ kcal/mol), resulting in the decay of the photocatalyst to **5CzBn** and reaching ^{T}**10**, in which a reductive

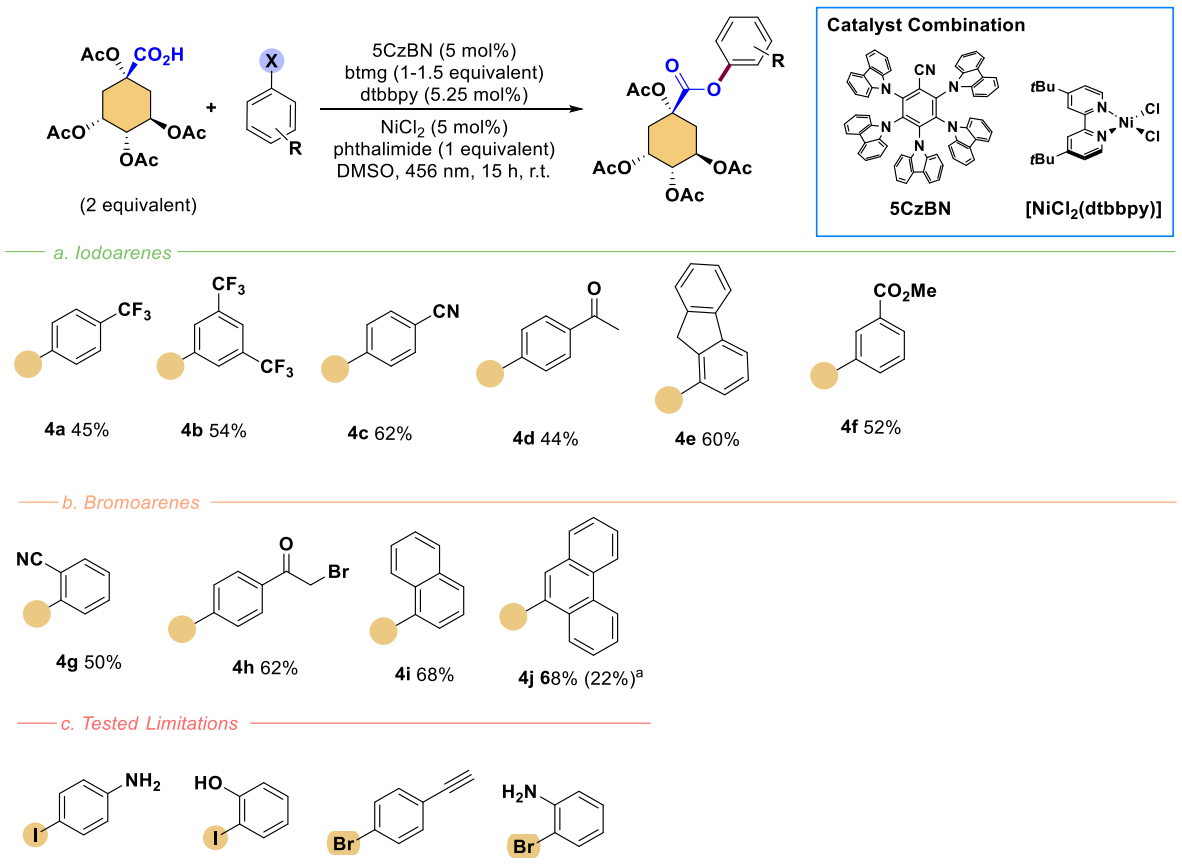

Scheme 2. Scope of TAQA decarboxylative arylation. Yields determined by ^{1}H NMR using 1,3,5-trimethoxybenzene as internal standard. [a)] in parenthesis, isolated yield from reaction with 1 mmol of TAQA.

elimination process is more likely than for ^{S}**10**. The smaller energy barrier for the reductive elimination from Ni(II), upon the energy transfer process, is analogous to what was previously described for the Ir/Ni metallaphotoredox dual catalysis [35a]. In the present system, although the origin of the **5CzBN*** triplet state being unstudied, the formation of ^{T}**10** is advanced to happen through a MLCT upon energy transfer from the excited photocatalyst to the Ni(II) species. Upon reduction of the nickel complex, and relaxation of the metal complex to the singlet state, the T-distorted ^{S}**11** complex keeps a Ni–C interaction ($d_{Ni\text{-}C} = 2.07$ Å), while the interaction of the metal with the oxygen atom becomes considerably weaker ($d_{Ni\text{-}O} = 2.12$ Å in ^{T}**11** vs $d_{Ni\text{-}O} = 2.44$ Å in ^{S}**11**). Release of the ester and taking of another iodo arene molecule releases the nickel(0) η^2 complex **5** to renew the catalytic cycle.

In order to better understand the lack of formation of decarboxylative arylation products, a mechanism based on literature precedents for the nickel-catalyzed C(sp^3)-C(sp^2) cross-coupling was considered. The proposed mechanism follows previous reports on an operative Ni (I)/Ni(III) catalytic cycle, resulting from the Ni(0)/Ni(II) comproportionation [40] or photocatalytic reduction [40,41] of the Ni(II) initial species. The energy barriers for the oxidative addition and reductive elimination of *N*-coordinated Ni(I)/Ni(III) pairs were determined to be a more facile process than a Ni(0)/Ni(II) catalytic cycle [42], suggesting a mechanism based on the catalytic turnover of a Ni(I) species. Thus, a mechanism starting from $Ni^{I}Cl$•bpy that undergoes addition to the radical derived from quinate oxidation and decarboxylation, followed by oxidative addition and reductive elimination, is presented as a reasonable pathway to describe the formation of C-arylated QA derivative (Figs. S7–S9 in Supporting Information). The hypothesized Ni^{I}–Ni^{II}–Ni^{I}–Ni^{III}–Ni^{I} cycle presented involves two SET processes that are only slightly endergonic (5.5 kcal/mol). Moreover, the most energy-demanding species is only 4.8 kcal/mol higher than the initial pair or reactants considered and corresponds to the radical addition transition state (Fig. S7). The remaining mechanism is characterized by a series of events that are overall highly exergonic (−88.8 kcal/mol), with the reductive elimination step having the higher energy barrier in the process (13.0 kcal/mol) and being the rate-determining step as identified in other studies [31].

In view of the favorable process described for the Ni-catalyzed decarboxylative arylation, we then looked into the photocatalytic cycle. It is known that the photoredox catalyst **5CzBN** undergoes excitation with visible light to its triplet state due to the well-separated HOMO and LUMO. Nevertheless, the ΔE_{ST} gap is small enough to allow reverse intersystem crossing [43]. Carbazolyl cyanobenzene-based photocatalysts generally exhibit strong oxidative and reductive capabilities comparable to many metal complexes. Nevertheless, the photoredox potentials of **5CzBN** show its ability to act as a reducing agent ($E_{1/2}(*P/P^{-}) = +1.20$ V; $E_{1/2}(P^{+}/*P) = -1.35$ V) [44], in opposition to most cyanoarenes known for undergoing reductive quenching of the photoexcited states [45]. With that in mind, the quenching of the photocatalyst through a reductive or oxidative cycle was investigated by DFT (Fig. S5). Comparison of the reductive and oxidative quenching cycles show a strong preference for the latter when comparing the energy barriers of single electron transfers. Notwithstanding that the photocatalyst quenching is slightly endergonic (ΔG = 2.3 kcal/mol), an energy barrier of 25.1 kcal/mol still needs to be overcome to promote quinate oxidation. The comparison of the two mechanism pathways considered suggests that the *O*-arylation path is independent of the photoredox potential of the photocatalyst, as it acts as a photosensitizer to participate in the energy transfer to the nickel intermediate species. Such a conclusion is also supported by the fact that screening of photocatalysts of different redox potentials did not change the reaction outcome.

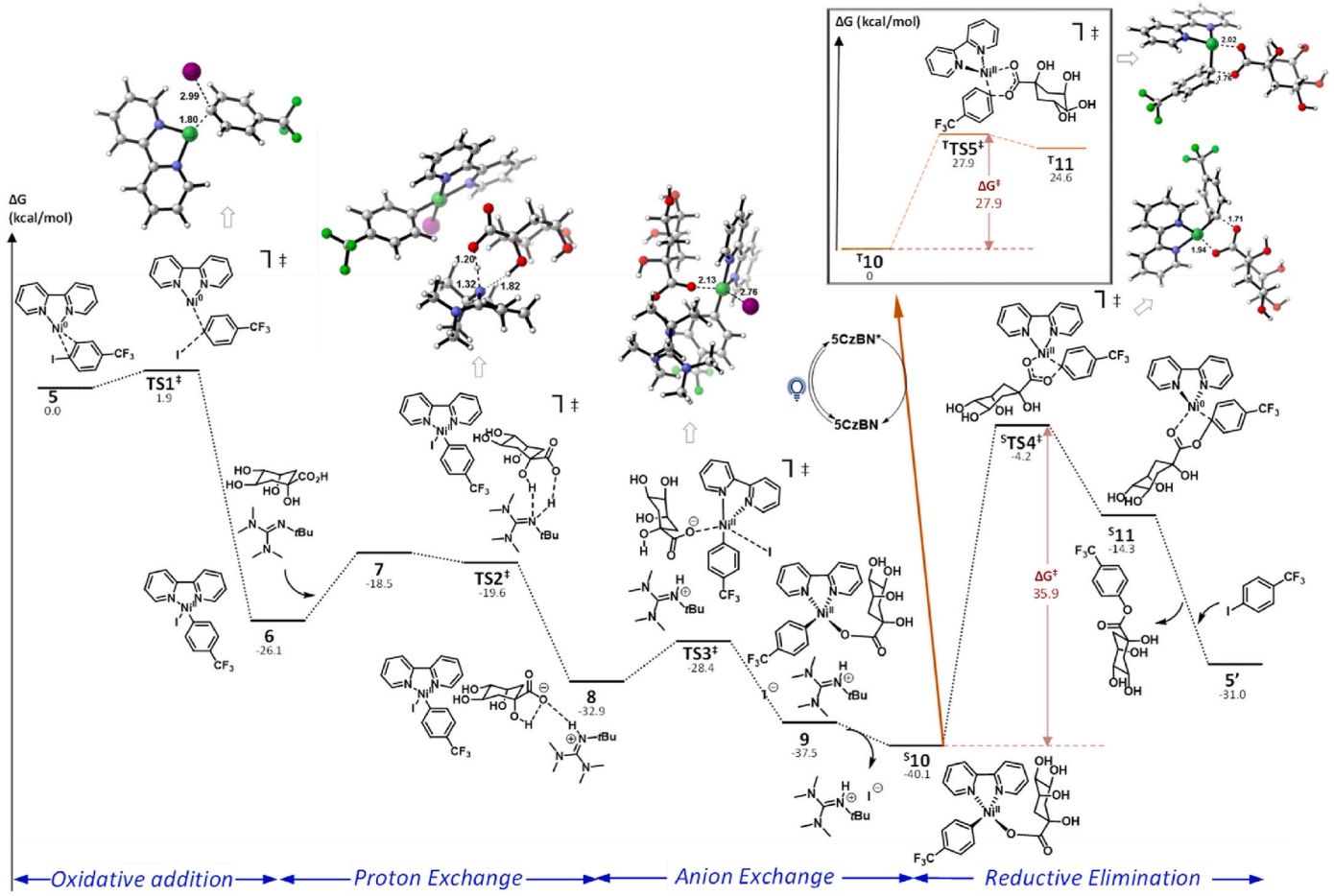

Fig. 1. Calculated energetics for the nickel-catalyzed *O*-arylation of QA. Gibbs free energies were computed at the BP86(PCM-DMSO)/(SDD,6-31+G**) level of theory.

Despite the low energetic barriers determined for the *O*-arylation process, the presence of Ni species in different oxidation states than the one considered here cannot be ruled out due to the recent reports on the ability of the nickel complexes to reach photoexcited states [46].

3. Conclusion

In conclusion, a mild, fast, and selective method for the construction of QA-derived esters, surpassing the use of protecting groups was successfully developed. The *O*-arylation of QA results in the construction of a new O–C(sp^2) bond in naturally abundant QA, applicable to a range of aryl halides, thus expanding the QA-derived chemical space. The employed purely organic photocatalyst, and the catalytically active nickel complex is prepared *in situ* from an inexpensive nickel source. The boundaries on the aryl halide scope have been set to the required presence of electron-withdrawing substituents, but the reaction was nevertheless shown to be amenable to the introduction of heterocyclic moieties. A computational study on the transformation suggests an operative Ni catalytic cycle consisting of oxidative addition, anion exchange and reductive elimination, with this last step taking place after energy transfer from the photocatalyst to the Ni(II) species. A comparison of the proposed *O*-arylation mechanism with a decarboxylative arylation one indicates that the required single electron transfer processes of the latter are considerably more energy-demanding. This rules out a decarboxylative arylation mechanism despite this being the Ni-catalyzed favorable pathway.

4. Experimental section

General Information: All solvents were distilled prior to use and, when mentioned, dried over standard drying agents according to the usual procedures. Dry tetrahydrofuran (THF) and dichloromethane (DCM) were obtained from INERT PureSolv micro apparatus. Anhydrous tetrahydrofuran was freshly distilled before use in order to remove the radical inhibitor BHT present as a stabilizer. DMSO was dried by standing in freshly activated 3 Å molecular sieves (20 % w/v). 3 Å molecular sieves were supplied by Sigma-Aldrich and activated before use. Activation of the MS was performed in a 400 °C oven for 4 h. DMF was supplied by Aldrich in Sureseal® bottles. All the reagents were purchased from commercial sources (Sigma-Aldrich, Alfa Aesar, Fluorochem, Acros, TCI) and used without further purification unless specified.

All reactions were set up under an argon atmosphere in oven-dried glassware using freeze-pump-thaw cycling. The reaction mixtures, placed in Rotaflo® stopcock equipped Schlenk tubes of 0.95 cm internal diameter, were irradiated using three Kessil® PR160L@456 nm lamps, equipped with a cooling fan, according to the set-up picture shown in the supplementary material. The fan speed was set such that the reaction temperature did not go over 30 °C. Reaction mixtures were analyzed by thin layer chromatography (TLC) using Merck silica gel 60F254 aluminum plates and visualized by UV light and stained with potassium permanganate ($KMnO_4$) or a ceric ammonium molybdate (CAM) stain. Thin-layer chromatography (TLC) was carried out on Kieselgel 60HF254 from Merck Co. and used to monitor the reaction progress. Separation and purification of compounds by flash column chromatography (FCC)

was performed using Kieselgel 60 (230–400 mesh, Merck).

^{1}H and ^{13}C NMR spectra were acquired on a Bruker MX300 spectrometer. Chemical shifts are reported in ppm from TMS with the solvent resonance as the internal standard ($CHCl_3$: $\delta = 7.27$ ppm for ^{1}H NMR and $\delta = 77.0$ ppm for ^{13}C NMR). Data are reported as follows: chemical shift (δ), multiplicity (s = singlet, d = doublet, t = triplet, q = quartet, dd = doublet of doublets, m = multiplet), coupling constants (Hz). ^{19}F NMR spectra were acquired on a Bruker Fourier 400. The Liquid chromatography–mass spectrometry (LC-MS) was realized using a Dionex Ultimate 3000 UHPLC + system equipped with a Multiple-Wavelength detector, using an imChem Surf C18 TriF 100A 3 μm 100 × 2.1 mm column coupled to a Thermo Scientific Q Exactive hybrid quadrupole-Orbitrap mass spectrometer (Thermo ScientificTM Q ExactiveTM Plus). The mass spectrometry was performed using the previously mentioned mass spectrometer. Tetraacetyl quinic acid (TAQA) was prepared from quinic acid according to a previously reported procedure [47]. The photocatalysts were obtained according to previously established procedures, namely 3DPAFIPN, 4CZIPN, and 5CZIPN, with similar spectral characterization as there described [45c].

General Procedure for quinic acid (QA)* O-*arylation: A flame-dried 10 mL Schlenk tube, equipped with a Rotaflo® stopcock, magnetic stirring bar and an argon supply tube, was firstly charged under argon with $NiCl_2$.Glyme (2.2 mg, 0.01 mmol, 5 mol%). The tube was then charged with 4-iodobenzotrifluoride (54.4 mg, 0.2 mmol, 1 equiv.), 5CzBN (1.9 mg, 0.002 mmol, 1 mol%), 2,2′-bipyridine (bpy, 1.64 mg, 0.0105 mmol, 5.25 mol%), phthalimide (29.4 mg, 0.2 mmol, 1 equiv.) and QA (76.9 mg, 0.4 mmol, 2 eq) followed by anhydrous DMSO (2 mL). The reaction mixture was vigorously stirred for 5 min, after which 2-*tert*-butyl-1,1,3,3-tetramethylguanidine (btmg, 68.4 mg, 0.4 mmol, 2 equiv.) was added, the reaction mixture was further subjected to a freeze-pump-thaw procedure (three cycles), and the vessel was refilled with argon. The reaction mixture was irradiated under vigorous stirring for 15 h. After that, the reaction mixture was quenched with water (approx. 2 mL) and extracted with EtOAc (4 × 3 mL). Trimethoxybenzene (tmb, 1.2 mg, 0.067 mmol) was added as an internal standard, and the solvent was removed under reduced pressure, followed by dissolution in DMSO-d_6 and ^{1}H NMR analysis to determine the reaction yield.

4-trifluoromethylphenyl quinate **(2):** ^{1}H NMR (300 MHz, DMSO-d_6) δ 7.62 (d, $J = 8.6$ Hz, 2H), 6.99 (d, $J = 8.5$ Hz, 2H), 4.61 (s, 1H), 4.26 (s, 1H), 4.04–3.94 (m, 1H), 3.85 (td, $J = 6.3$, 3.5 Hz, 1H), 3.42 (dd, $J = 6.2$, 3.0 Hz, 1H), 2.29–1.91 (m, 4H); ^{13}C{1H} NMR (75 MHz, DMSO-d_6) δ 177.5, 158.1, 135.6, 127.7, 127.6, 124.3, 118.8, 83.2, 75.1, 69.6, 66.8, 38.7, 35.7; ESI-HRMS calcd for $C_{14}H_{15}F_3O_6$ $[M+H]^+$, 337.2707; found 337.0886.

***General Procedure for* tetraacetate quinic acid (*TAQA*) O-*arylation*:** A flame-dried 10 mL Schlenk tube, equipped with a Rotaflo® stopcock, magnetic stirring bar and an argon supply tube, was firstly charged under argon with $NiCl_2$ (1.3 mg, 0.01 mmol, 5 mol%). The tube was then charged with the aryl halide (0.2 mmol), 5CzBN (1.9 mg, 0.002 mmol, 1 mol%), 4,4′-di-*tert*-butyl-2,2′-dipyridyl (dtbbpy, 2.81 mg, 0.0105 mmol, 5.25 mol%.), phthalimide (29.4 mg, 0.2 mmol, 1 equiv.) and **TAQA** (**3**) (144 mg, 0.4 mmol, 2 equiv.) followed by anhydrous DMSO (2 mL). The reaction mixture was vigorously stirred for 5 min, after which btmg (68.4 mg, 0.4 mmol, 2 equiv.) was added, the reaction mixture was further subjected to a freeze-pump-thaw procedure (three cycles), and the vessel was refilled with argon. The reaction mixture was irradiated under vigorous stirring for 15 h. After that, the reaction mixture was quenched with water (approx. 2 mL) and extracted with EtOAc (4 × 3 mL). The combined organic layers were washed (3 × 1 mL) with an aqueous solution of NaOH (1 % w/v), washed with brine, dried over anhydrous Mg_2SO_4 and filtered. Trimethoxybenzene (tmb, 1.2 mg, 0.067 mmol) was added as an internal standard, and the solvent was removed under reduced pressure, followed by dissolution in $CDCl_3$ and ^{1}H NMR analysis to determine the reaction yield. The mixture was purified by flash column chromatography or preparative TLC (PTLC) using *n*-Hexane:EtOAc (30–50 % of EtOAc) as eluent to obtain pure compound for spectral characterization.

4-trifluoromethylphenyl tetraacetyl quinate (**4a**)**:** Obtained in 45 % according to ^{1}H NMR analysis, isolated as a pale oil after purification by PTLC (40 % EtOAC in Hexane), ^{1}H NMR (300 MHz, $CDCl_3$) δ 7.64 (d, $J =$ 8.6 Hz, 2H), 7.20 (d, $J = 9.0$, 2H), 5.62 (q, $J = 3.8$ Hz, 1H), 5.48 (td, $J =$ 9.8, 4.3 Hz, 1H), 5.07 (dd, $J = 9.5$, 3.5 Hz, 1H), 2.77–2.64 (m, 2H), 2.50 (dd, $J = 15.7$, 3.8 Hz, 1H), 2.17 (s, 3H), 2.09 (s, 3H), 2.04 (s, 3H), 2.03 (s, 3H); ^{13}C{1H} NMR (75 MHz, $CDCl_3$) δ 170.1, 170.1, 170.0, 169.9, 168.9, 153.0, 129.4, 129.3, 129.0, 128.5, 127.1, 127.1, 127.02, 126.97, 125.7, 122.1, 121.8, 78.6, 77.4, 71.3, 67.5, 66.6, 36.5, 32.2, 29.8, 21.07, 21.05, 21.03, 20.8; ^{19}F{1H} NMR (376 MHz, $CDCl_3$) δ −62.3; ESI-HRMS calcd for $C_{22}H_{27}F_3O_{10}N$ $[M + NH_4]^+$: 522.1582, found 522.1570.

3,5-di(trifluoromethyl)phenyl tetraacetyl quinate (**4b**)**:** Obtained in 54 % according to ^{1}H NMR analysis, isolated as a pale oil after purification by PTLC (40 % EtOAC in Hexane). ^{1}H NMR (300 MHz, $CDCl_3$) δ 7.77 (s, 1H), 7.54 (s, 2H), 5.62 (q, $J = 3.9$ Hz, 1H), 5.47 (td, $J = 9.7$, 4.3 Hz, 1H), 5.08 (dd, $J = 9.4$, 3.5 Hz, 1H), 2.77–2.62 (m, 2H), 2.51 (dd, $J = 15.5$, 3.7 Hz, 1H), 2.19 (s, 3H), 2.09 (s, 3H), 2.04 (s, 3H), 2.03 (s, 3H); ^{13}C{1H} NMR (75 MHz, $CDCl_3$) δ 170.3, 170.1, 170.0, 169.9, 168.7, 150.9, 133.9, 133.4, 133.0, 132.5, 128.1, 124.5, 122.3, 120.9, 120.3, 117.3, 78.4, 71.0, 67.3, 66.5, 36.4, 32.1, 29.8, 21.1, 21.0, 20.8; ^{19}F{1H} NMR (376 MHz, $CDCl_3$) δ −62.9; ESI-HRMS calcd for $C_{23}H_{26}F_6O_{10}N$ $[M + NH_4]^+$: 590.1455; found 590.1443.

4-cyanophenyl tetraacetyl quinate (**4c**)**:** Obtained in 62 % according to ^{1}H NMR analysis, isolated as a pale oil after purification by PTLC (40 % EtOAC in Hexane). ^{1}H NMR (300 MHz, $CDCl_3$) δ 7.69 (d, $J = 9.0$, 2H), 7.21 (d, $J = 9.0$, 2H), 5.61 (q, $J = 3.9$ Hz, 1H), 5.46 (td, $J = 9.8$, 4.3 Hz, 1H), 5.06 (dd, $J = 9.4$, 3.5 Hz, 1H), 2.77–2.60 (m, 2H), 2.48 (dd, $J =$ 15.7, 3.8 Hz, 1H), 2.17 (s, 3H), 2.09 (s, 3H), 2.03 (s, 3H), 2.02 (s, 3H); ^{13}C{1H} NMR (75 MHz, $CDCl_3$) δ 170.2, 170.1, 170.0, 169.9, 168.6, 153.6, 133.9, 122.5, 118.2, 110.4, 78.5, 71.1, 67.4, 66.5, 36.4, 32.1, 21.1, 21.0, 20.8; ESI-HRMS calcd for $C_{22}H_{27}N_2O_{10}$ $[M + NH_4]^+$: 479.1660; found 479.1651.

4-acetylphenyl tetraacetyl quinate (**4d**)**:** Obtained in 44 % according to ^{1}H NMR analysis, isolated as a pale oil after purification by PTLC (40 % EtOAC in Hexane). ^{1}H NMR (300 MHz, $CDCl_3$) δ 7.97 (d, $J = 9.0$, 2H), 7.15 (d, $J = 9.0$, 2H), 5.61 (q, $J = 3.6$ Hz, 1H), 5.47 (td, $J = 9.9$, 4.3 Hz, 1H), 5.06 (dd, $J = 9.5$, 3.5 Hz, 1H), 2.78–2.61 (m, 2H), 2.58 (s, 3H), 2.49 (dd, $J = 15.8$, 3.6 Hz, 1H), 2.17 (s, 3H), 2.09 (s, 3H), 2.03 (s, 3H), 2.02 (s, 3H); ^{13}C{1H} NMR (75 MHz, $CDCl_3$) δ 196.9, 170.13, 170.11, 170.0, 169.9, 168.8, 154.0, 135.2, 130.1, 121.5, 78.6, 71.2, 67.4, 66.5, 36.5, 32.1, 29.6, 26.8, 21.09, 21.07, 21.04, 20.8; ESI-HRMS calcd for $C_{23}H_{30}O_{11}N$ $[M + NH_4]^+$: 496.1813; found 496.1812.

9H-fluoren-2-yl *tetraacetyl quinate* (**4e**)**:** Obtained in 60 % according to ^{1}H NMR analysis, isolated as a pale oil after purification by PTLC (40 % EtOAC in Hexane); ^{1}H NMR (300 MHz, $CDCl_3$) δ 7.74 (d, $J = 8.0$ Hz, 2H), 7.52 (d, 1H), 7.41–7.26 (m, 3H), 7.06 (dd, $J = 8.3$, 2.2 Hz, 1H), 5.64 (q, $J = 3.7$ Hz, 1H), 5.52 (td, $J = 10.0$, 4.3 Hz, 1H), 5.09 (dd, $J =$ 9.6, 3.5 Hz, 1H), 3.88 (s, 2H), 2.82–2.71 (m, 2H), 2.53 (dd, $J = 15.9$, 3.7 Hz, 1H), 2.20 (s, 3H), 2.11 (s, 3H), 2.05 (s, 6H); ^{13}C{1H} NMR (75 MHz, $CDCl_3$) δ 170.09, 170.06, 170.0, 169.9, 169.4, 149.5, 144.8, 143.4, 140.9, 140.1, 127.0, 126.9, 125.1, 120.5, 120.0, 119.7, 118.2, 78.8, 71.5, 67.7, 66.6, 37.0, 36.7, 32.2, 21.2, 21.1, 21.0, 20.8; ESI-HRMS calcd for $C_{28}H_{32}O_{10}N$ $[M + NH_4]^+$ 542.2021; found 542.2014.

3-carbomethoxyphenyl tetraacetyl quinate (**4f**)**:** Obtained in 52 % according to 1H NMR analysis, isolated as a pale oil after purification by PTLC (40 % EtOAC in Hexane); ^{1}H NMR (300 MHz, $CDCl_3$) δ 7.93 (dt, $J =$ 7.8, 1.3 Hz, 1H), 7.74–7.70 (m, 1H), 7.46 (t, $J = 7.9$ Hz, 1H), 7.31–7.27 (m, 1H), 5.63 (q, $J = 3.8$ Hz, 1H), 5.50 (td, 1H), 5.08 (dd, $J =$ 9.5, 3.5 Hz, 1H), 3.92 (s, 3H), 2.79–2.67 (m, 2H), 2.51 (dd, $J = 15.7$, 3.7 Hz, 1H), 2.18 (s, 3H), 2.10 (s, 3H), 2.05 (s, 3H), 2.04 (s, 3H). ^{13}C NMR (75 MHz, $CDCl_3$) δ 170.11, 170.07, 170.04, 169.88, 169.07, 166.12, 150.44, 131.98, 129.74, 127.65, 126.02, 122.44, 78.67, 77.36, 71.37, 67.59, 66.61, 52.50, 36.65, 32.19, 29.84, 21.12, 21.07, 20.83, 1.16; ESI-HRMS calcd for $C_{23}H_{30}O_{12}N$ $[M + NH_4]^+$, 512.1763; found 512.1760.

2-cyanophenyl tetraacetyl quinate (**4g**)**:** Obtained in 50 % according to

^{1}H NMR analysis, isolated as a pale oil after purification by PTLC (40 % EtOAC in Hexane); ^{1}H NMR (300 MHz, $CDCl_3$) δ 7.72–7.57 (m, 2H), 7.42–7.23 (m, 2H), 5.62 (q, J = 3.6 Hz, 1H), 5.54 (td, J = 10.3, 4.4 Hz, 1H), 5.05 (dd, J = 9.9, 3.6 Hz, 1H), 2.88–2.69 (m, 2H), 2.50 (dd, J = 16.0, 3.6 Hz, 1H), 2.21 (s, 3H), 2.10 (s, 3H), 2.05 (s, 3H), 2.02 (s, 3H); ^{13}C{1H} NMR (75 MHz, $CDCl_3$) δ 170.4, 170.13, 170.07, 169.9, 168.2, 151.7, 134.4, 133.4, 126.9, 123.1, 114.9, 106.8, 78.6, 71.6, 67.5, 66.1, 36.6, 32.2, 21.13, 21.10, 20.8; ESI-HRMS calcd for $C_{22}H_{27}N_2O_{10}$ [M + NH_4]$^+$: 479.1660; found 479.1649.

4-(α-bromoacetyl)phenyl tetraacetyl quinate (**4h**)**:** Obtained in 62 % according to ^{1}H NMR analysis, isolated as a pale oil after purification by PTLC (40 % EtOAC in Hexane); ^{1}H NMR (300 MHz, $CDCl_3$) δ 7.71 (d, J = 9.0, 2H), 7.62 (d, J = 9.0, 2H), 5.57 (q, J = 3.4 Hz, 1H), 5.49 (td, 1H), 5.30 (dd, 2H), 5.01 (dd, J = 10.2, 3.6 Hz, 1H), 2.81–2.68 (m, 2H), 2.43 (dd, J = 16.1, 3.5 Hz, 1H), 2.13 (s, 4H), 2.06 (s, 3H), 2.04 (s, 3H), 1.99 (s, 3H); ^{13}C{1H} NMR (75 MHz, $CDCl_3$) δ 190.6, 170.2, 170.1, 170.0, 169.9, 169.7, 132.6, 132.4, 129.5, 129.3, 78.8, 72.0, 67.7, 66.5, 66.3, 37.2, 31.9, 29.6, 21.2, 21.1, 20.8; ESI-HRMS calcd for $C_{23}H_{29}BrO_{11}N$ [M + NH_4]$^+$: 574.09161; found 574.0916.

1-naphthyl tetraacetyl quinate (**4i**)**:** Obtained in 68 % according to ^{1}H NMR analysis, isolated as a pale oil after purification by PTLC (40 % EtOAC in Hexane); ^{1}H NMR (300 MHz, $CDCl_3$) δ 7.92–7.79 (m, 2H), 7.74 (d, J = 1.0 Hz, 1H), 7.59–7.44 (m, 2H), 7.44 (t, J = 7.9 Hz, 1H), 7.21 (dd, J = 7.6, 1.1 Hz, 1H), 5.66 (q, J = 3.7 Hz, 1H), 5.58 (td, J = 10.2, 4.4 Hz, 1H), 5.11 (dd, J = 9.8, 3.6 Hz, 1H), 2.99–2.85 (m, 1H), 2.59 (dd, J = 15.9, 3.6 Hz, 1H), 2.22 (s, 4H), 2.12 (s, 3H), 2.05 (s, 6H); ^{13}C{1H} NMR (75 MHz, $CDCl_3$) δ 170.18, 170.15, 170.1, 169.9, 169.2, 146.3, 134.7, 128.1, 126.8, 126.7, 126.5, 125.4, 120.9, 117.7, 79.0, 71.6, 67.6, 66.4, 37.0, 36.2, 32.2, 29.57, 21.2, 21.1, 20.8; ESI-HRMS calcd for $C_{25}H_{30}O_{10}N$ [M + NH_4]$^+$: 504.1864; found 504.1862.

9-phenanthrenyl tetraacetyl quinate (**4j**)**:** Obtained in 68 % according to ^{1}H NMR analysis, isolated as a pale oil after purification by PTLC (40 % EtOAC in Hexane); ^{1}H NMR (300 MHz, $CDCl_3$) δ 8.70 (d, J = 7.0, 1H), 8.65 (d, J = 8.4, 1H), 7.93 (dd, J = 7.9, 1.7 Hz, 1H), 7.85 (dd, J = 7.3, 2.0 Hz, 1H), 7.75–7.56 (m, 4H), 7.50 (s, 1H), 5.69 (q, J = 3.7 Hz, 1H), 5.61 (td, J = 10.3, 4.4 Hz, 1H), 5.14 (dd, J = 9.8, 3.5 Hz, 1H), 2.95 (m, J = 13.7, 7.2, 3.2 Hz, 2H), 2.64 (dd, J = 15.9, 3.6 Hz, 1H), 2.25 (s, 4H), 2.14 (s, 3H), 2.06 (s, 6H); ^{13}C{1H} NMR (75 MHz, $CDCl_3$) δ 170.3, 170.2, 170.1, 170.0, 169.3, 144.7, 131.6, 131.4, 129.1, 128.7, 127.5, 127.3, 127.2, 126.8, 126.3, 123.1, 122.8, 121.7, 117.5, 79.1, 71.7, 67.7, 66.5, 37.1, 32.3, 21.3, 21.1, 20.9; ESI-HRMS calcd for $C_{25}H_{30}O_{10}N$ [M + NH_4]$^+$: 554.2021; found 554.2015.

CRediT authorship contribution statement

Miguel A. Bárbara: Writing – review & editing, Methodology, Investigation. **Nuno R. Candeias:** Writing – review & editing, Writing – original draft, Supervision, Project administration, Investigation, Conceptualization. **Luis F. Veiros:** Writing – review & editing, Supervision. **Filipe Menezes:** Writing – review & editing, Data curation. **Andrea Gualandi:** Writing – review & editing, Supervision. **Pier G. Cozzi:** Writing – review & editing, Supervision. **Carlos A.M. Afonso:** Writing – review & editing, Supervision.

Declaration of competing interest

The authors declare the following financial interests/personal relationships which may be considered as potential competing interests: Nuno Filipe Rafael Candeias reports financial support was provided by Foundation for Science and Technology. Carlos A. M. Afonso reports financial support was provided by Foundation for Science and Technology. Luis F. Veiros reports financial support was provided by Foundation for Science and Technology. If there are other authors, they declare that they have no known competing financial interests or personal relationships that could have appeared to influence the work reported in this paper.

Acknowledgments

This work received financial support from PT national funds (FCT/MCTES, Fundação para a Ciência e Tecnologia and Ministério da Ciência, Tecnologia e Ensino Superior) through the projects PTDC/QUI-QOR/1131/2020, UIDB/04138/2020 | UIDP/04138/2020 and UIDB/50006/2020 | UIDP/50006/2020. NRC further acknowledges FCT for financial support under the Scientific Employment Stimulus (CEECINST/2018). CSC–IT Center for Science Ltd, Finland is acknowledged for the allocation of computational resources. Centro de Química Estrutural (CQE) and Institute of Molecular Sciences (IMS) also acknowledge the financial support of FCT/MCTES (Projects UIDB/00100/2020, UIDP/00100/2020, and LA/P/0056/2020, respectively).

Appendix A. Supplementary data

Supplementary data to this article can be found online at https://doi.org/10.1016/j.tgchem.2025.100070.

Data availability

Data will be made available on request.

References

[1] S. Parmaki, F.C. Ferreira, T. Esteves, C.A.M. Afonso, M. Koutinas, in: S. Varjani, A. Pandey, T. Bhaskar, S.V. Mohan, D.C.W. Tsang (Eds.), Biomass, Biofuels, Biochemicals: Circular Bioeconomy: Technologies for Biofuels and Biochemicals, Elsevier Inc. All, 2022, pp. 295–335.
[2] a) F. Allais, Curr. Opin. Green Sustainable Chem. 40 (2023);
b) H. Zhu, Y. Cai, S. Ma, Y. Futamura, J. Li, W. Zhong, X. Zhang, H. Osada, H. Zou, ChemSusChem 14 (2021) 5320–5327.
[3] A. Antenucci, S. Dughera, P. Renzi, ChemSusChem 14 (2021) 2785–2853.
[4] a) R.A. Fernandes, P. Kumar, P. Choudhary, Eur. J. Org. Chem. 2021 (2020) 711–740;
b) R.A. Fernandes, P. Kumar, P. Choudhary, Chem. Commun. 56 (2020) 8569–8590.
[5] A. Gogoi, Mezhubeinuo, S. Nongrum, G. Bez, Curr. Org. Chem. 25 (2021) 1566–1610.
[6] a) D. Wianowska, M. Gil, Phytochem. Rev. 18 (2018) 273–302;
b) M.N. Clifford, I.B. Jaganath, I.A. Ludwig, A. Crozier, Nat. Prod. Rep. 34 (2017) 1391–1421;
c) N. Yuda, M. Tanaka, M. Suzuki, Y. Asano, H. Ochi, K. Iwatsuki, J. Food. Sci. 77 (2012) H254–H261;
d) L. Grunovaitė, M. Pukalskienė, A. Pukalskas, P.R. Venskutonis, J. Funct.Foods 24 (2016) 85–96;
e) J. Wang, D. Lu, Q. Sun, H. Zhao, X. Ling, P. Ouyang, Chem. Eng. Sci. 78 (2012) 53–62;
f) O. Santana-Méridas, A. González-Coloma, R. Sánchez-Vioque, Phytochem. Rev. 11 (2012) 447–466;
g) M.I. Sifola, L. Carrino, E. Cozzolino, L. del Piano, G. Graziani, A. Ritieni, Sustainability 13 (2021) 2087.
[7] E. Arceo, J.A. Ellman, R.G. Bergman, ChemSusChem 3 (2010) 811–813.
[8] a) B. Assoah, L.F. Veiros, C.A.M. Afonso, N.R. Candeias, Eur. J. Org. Chem. (2016) 3856–3861;
b) N. Ran, D.R. Knop, K.M. Draths, J.W. Frost, J. Am. Chem. Soc. 123 (2001) 10927–10934.
[9] T. Pfennig, J.M. Carraher, A. Chemburkar, R.L. Johnson, A.T. Anderson, J.-P. Tessonnier, M. Neurock, B.H. Shanks, Green Chem. 19 (2017) 4879–4888.
[10] a) S. Wu, W. Chen, S. Lu, H. Zhang, L. Yin, Molecules 27 (2022) 4779;
b) E. Valanciene, N. Malys, Antioxidants 11 (2022) 2427;
c) N.R. Candeias, B. Assoah, S.P. Simeonov, Chem. Rev. 118 (2018) 10458–10550.
[11] a) V. Enev, in: E.M. Carreira, H. Yamamoto (Eds.), Comprehensive Chirality, Elsevier, Amsterdam, 2012, pp. 325–345;
b) A. Barco, S. Benetti, C.D. Risi, P. Marchetti, G.P. Pollini, V. Zanirato, Tetrahedron Asymmetry 8 (1997) 3515–3545;
c) J. Mulzer, M. Drescher, V.S. Enev, Curr. Org. Chem. 12 (2008) 1613–1630.
[12] R. Altmann, H. Falk, Monatsh. Chem. 126 (1995) 1225–1232.
[13] D.H. Hua, K. Lou, J. Havens, E.M. Perchellet, Y. Wang, J.-P. Perchellet, T. Iwamoto, Tetrahedron 60 (2004) 10155–10163.
[14] D. Magdziak, G. Lalic, H.M. Lee, K.C. Fortner, A.D. Aloise, M.D. Shair, J. Am. Chem. Soc. 127 (2005) 7284–7285.
[15] M. Frank, R. Miethchen, Carbohydr. Res. 313 (1998) 49–53.
[16] a) N.A. Romero, D.A. Nicewicz, Chem. Rev. 116 (2016) 10075–10166;
b) A.Y. Chan, I.B. Perry, N.B. Bissonnette, B.F. Buksh, G.A. Edwards, L.I. Frye, O. L. Garry, M.N. Lavagnino, B.X. Li, Y. Liang, E. Mao, A. Millet, J.V. Oakley, N. L. Reed, H.A. Sakai, C.P. Seath, D.W.C. MacMillan, Chem. Rev. 122 (2022) 1485–1542;

c) N.E.S. Tay, D. Lehnherr, T. Rovis, Chem. Rev. 122 (2022) 2487–2649;
d) M.J.P. Mandigma, J. Kaur, J.P. Barham, ChemCatChem 15 (2023);
e) S.B. Beil, S. Bonnet, C. Casadevall, R.J. Detz, F. Eisenreich, S.D. Glover, C. Kerzig, L. Naesborg, S. Pullen, G. Storch, N. Wei, C. Zeymer, JACS Au 4 (2024) 2746–2766.
[17] G.E.M. Crisenza, P. Melchiorre, Nat. Commun. 11 (2020) 803.
[18] a) M. Cortes-Clerget, J. Yu, J.R.A. Kincaid, P. Walde, F. Gallou, B.H. Lipshutz, Chem. Sci. 12 (2021) 4237–4266;
b) V. Perchyonok, I. Lykakis, Curr. Org. Chem. 13 (2009) 573–598.
[19] a) Z. Huang, N. Luo, C. Zhang, F. Wang, Nat. Rev. Chem 6 (2022) 197–214;
b) T. Liu, J. Huang, J. Li, K. Wang, Z. Guo, H. Wu, S. Yang, H. Li, Green Chem. 25 (2023) 10338–10365;
c) D. Aboagye, R. Djellabi, F. Medina, S. Contreras, Angew. Chem. Int. Ed. Engl. 62 (2023) e202301909.
[20] J. Schwarz, B. König, Green Chem. 20 (2018) 323–361.
[21] J. Guo, D. Norris, A. Ramirez, J.L. Sloane, E.M. Simmons, J.M. Ganley, M. S. Oderinde, T.G.M. Dhar, G.H.M. Davies, T.C. Sherwood, ACS Catal. (2023) 11910–11918.
[22] C.N. Prieto Kullmer, J.A. Kautzky, S.W. Krska, T. Nowak, S.D. Dreher, D.W. C. MacMillan, Science 376 (2022) 532–539.
[23] E.R. Welin, C. Le, D.M. Arias-Rotondo, J.K. McCusker, D.W. MacMillan, Science 355 (2017) 380–385.
[24] C.D. McTiernan, X. Leblanc, J.C. Scaiano, ACS Catal. 8 (2018) 9847, 9847.
[25] C. Fischer, C. Kerzig, B. Zilate, O.S. Wenger, C. Sparr, ACS Catal. 10 (2019) 210–215.
[26] R. Sun, Y. Qin, D.G. Nocera, Angew. Chem. Int. Ed. Engl. 59 (2020) 9527–9533.
[27] Z. Zuo, D.T. Ahneman, L. Chu, J.A. Terrett, A.G. Doyle, D.W. MacMillan, Science 345 (2014) 437–440.
[28] J. Lu, B. Pattengale, Q. Liu, S. Yang, W. Shi, S. Li, J. Huang, J. Zhang, J. Am. Chem. Soc. 140 (2018) 13719–13725.
[29] E. Pinosa, E. Bassan, S. Cetin, M. Villa, S. Potenti, F. Calogero, A. Gualandi, A. Fermi, P. Ceroni, P.G. Cozzi, J. Org. Chem. 88 (2023) 6390–6400.
[30] M. Pitchai, A. Ramirez, D.M. Mayder, S. Ulaganathan, H. Kumar, D. Aulakh, A. Gupta, A. Mathur, J. Kempson, N. Meanwell, Z.M. Hudson, M.S. Oderinde, ACS Catal. 13 (2023) 647–658.
[31] K. Kolahdouzan, R. Khalaf, J.M. Grandner, Y. Chen, J.A. Terrett, M.P. Huestis, ACS Catal. 10 (2019) 405–411.
[32] a) D.A. Cagan, D. Bim, N.P. Kazmierczak, R.G. Hadt, ACS Catal. 14 (2024) 9055–9076;
b) S.I. Ting, W.L. Williams, A.G. Doyle, J. Am. Chem. Soc. 144 (2022) 5575–5582.
[33] H. Huang, J.L. Alvarez-Hernandez, N. Hazari, B.Q. Mercado, M.R. Uehling, ACS Catal. 14 (2024) 6897–6914.
[34] H. Beckurts, P. Echtermeier, Arch. Pharmazie 244 (1906) 37–57.
[35] a) Y.J. Dong, Z.W. Zhao, Y. Geng, Z.M. Su, B. Zhu, W. Guan, Inorg. Chem. 62 (2023) 1156–1164;
b) R.D. Bradley, B.D. McManus, J.G. Yam, V. Carta, A. Bahamonde, Angew. Chem. Int. Ed. Engl. 62 (2023) e202310753;
c) L. Tian, N.A. Till, B. Kudisch, D.W.C. MacMillan, G.D. Scholes, J. Am. Chem. Soc. 142 (2020) 4555–4559;
d) P. Ma, S. Wang, H. Chen, ACS Catal. 10 (2019) 1–6.
[36] a) J.N. Harvey, Annu. Rep. Prog. Chem., Sect. C 102 (2006) 203–226;
b) J.N. Harvey, in: N. Kaltsoyannis, J.E. McGrady (Eds.), Principles and Applications of Density Functional Theory in Inorganic Chemistry I, Springer Berlin Heidelberg, Berlin, Heidelberg, 2004, pp. 151–184.
[37] M. Yuan, Z. Song, S.O. Badir, G.A. Molander, O. Gutierrez, J. Am. Chem. Soc. 142 (2020) 7225–7234.
[38] B. Maity, C. Zhu, H. Yue, L. Huang, M. Harb, Y. Minenkov, M. Rueping, L. Cavallo, J. Am. Chem. Soc. 142 (2020) 16942–16952.
[39] J.B. Diccianni, T. Diao, Trends Chem. 1 (2019) 830–844.
[40] N.A. Till, S. Oh, D.W.C. MacMillan, M.J. Bird, J. Am. Chem. Soc. 143 (2021) 9332–9337.
[41] a) N.A. Till, L. Tian, Z. Dong, G.D. Scholes, D.W.C. MacMillan, J. Am. Chem. Soc. 142 (2020) 15830–15841;
b) H. Ren, G.-F. Li, B. Zhu, X.-D. Lv, L.-S. Yao, X.-L. Wang, Z.-M. Su, W. Guan, ACS Catal. 9 (2019) 3858–3865.
[42] I. Kalvet, Q. Guo, G.J. Tizzard, F. Schoenebeck, ACS Catal. 7 (2017) 2126–2132.
[43] S. Tanimoto, T. Suzuki, H. Nakanotani, C. Adachi, Chem. Lett. 45 (2016) 770–772.
[44] a) W. Ou, R. Zou, M. Han, L. Yu, C. Su, Chin. Chem. Lett. 31 (2020) 1899–1902;
b) T. Gandini, L. Dolcini, L. Di Leo, M. Fornara, A. Bossi, M. Penconi, A. Dal Corso, C. Gennari, L. Pignataro, ChemCatChem 14 (2022) e202200990.
[45] a) A. Tlili, S. Lakhdar, Angew. Chem. Int. Ed. Engl. 60 (2021) 19526–19549;
b) Y. Kwon, J. Lee, Y. Noh, D. Kim, Y. Lee, C. Yu, J.C. Roldao, S. Feng, J. Gierschner, R. Wannemacher, M.S. Kwon, Nat. Commun. 14 (2023) 92;
c) E. Speckmeier, T.G. Fischer, K. Zeitler, J. Am. Chem. Soc. 140 (2018) 15353–15365.
[46] a) S.I. Ting, S. Garakyaraghi, C.M. Taliaferro, B.J. Shields, G.D. Scholes, F. N. Castellano, A.G. Doyle, J. Am. Chem. Soc. 142 (2020) 5800–5810;
b) B.J. Shields, B. Kudisch, G.D. Scholes, A.G. Doyle, J. Am. Chem. Soc. 140 (2018) 3035–3039.
[47] C. Grandjean, C. Rommens, H. Gras-Masse, O. Melnyk, J. Chem. Soc. Perkin Trans. 1 (1999) 2967–2975.